



Accepted author manuscript (AAM)

Accepted: 16 April 2020

Published version:

Simonis S, Frank M, Krause MJ.

2020 On relaxation systems and their relation to discrete velocity Boltzmann models for scalar advection–diffusion equations.

Phil. Trans. R. Soc. A 378: 20190400.

<http://dx.doi.org/10.1098/rsta.2019.0400>

Subject Areas:

applied mathematics, differential equations

Keywords:

lattice Boltzmann methods, discrete velocity model, relaxation system, advection–diffusion equation

Author for correspondence:

Stephan Simonis

e-mail: stephan.simonis@kit.edu

On relaxation systems and their relation to discrete velocity Boltzmann models for scalar advection–diffusion equations

Stephan Simonis^{1,2}, Martin Frank^{2,3} and Mathias J. Krause^{1,2}

¹Lattice Boltzmann Research Group, Karlsruhe Institute of Technology, 76131 Karlsruhe, Germany

²Institute for Applied and Numerical Mathematics, Karlsruhe Institute of Technology, 76131 Karlsruhe, Germany

³Steinbuch Center for Computing, Karlsruhe Institute of Technology, 76344 Eggenstein-Leopoldshafen, Germany

The connection of relaxation systems and discrete velocity models is essential to the progress of stability as well as convergence results for lattice Boltzmann methods. In the present study we propose a formal perturbation ansatz starting from a scalar one-dimensional target equation, which yields a relaxation system specifically constructed for its equivalence to a discrete velocity Boltzmann model as commonly found in lattice Boltzmann methods. Further, the investigation of stability structures for the discrete velocity Boltzmann equation allows for algebraic characterizations of the equilibrium and collision operator. The methods introduced and summarized here are tailored for scalar, linear advection–diffusion equations, which can be used as a foundation for the constructive design of discrete velocity Boltzmann models and lattice Boltzmann methods to approximate different types of partial differential equations.

1. Introduction

The mesoscopic approach of lattice Boltzmann methods (LBM)—a well-established highly parallelizable tool in computational fluid dynamics (CFD)—is based on numerically solving a discrete velocity Boltzmann equation (DVBE) for particle density functions which are in turn averaged to obtain macroscopic variables as approximate solution of a target equation (TEQ). Mainly realized as a *bottom-up* track, the classical methodology consists of the proposal of an LBM, the proof of its limit towards the TEQ via asymptotic expansion techniques, and subsequent testing by means of numerical examples. As a consequence of this common procedure, the mathematical classification of the bidirectional relations between the ingredients of the employed LBM and significant attributes of the partial differential equation (PDE) to be numerically solved, is seldom addressed. Further, the recent trend towards application-selective enhancement of LBM—extending the basic method with deficiency-compensating techniques for specific test cases—often omits an in detail analysis concerning consistency, stability and convergence, and eventuates in a diversity of distinct LBM rather than an elaborated theoretical basis. The mathematical foundation of LBM seems to be incomplete, compared to the vast possibilities of analysis tools for conventional *top-down* methods, starting with a direct discretization of the PDE. Consequently, restrictive features due to stability issues in certain settings or critical sensitivity of the solution with respect to parameter choices persist.

Hence, a constructive procedure with a starting point at a given TEQ, ascertaining the possible LBM formulations for its numerical solution is of paramount interest. Mathematically rigorous and general treatments for this issue were proposed among others by Bouchut [5] and Junk [19], where the former publication focuses on Bhatnagar–Gross–Krook (BGK) [3] models for conservation laws and the latter, on constructing equilibrium distributions for kinetic schemes and LBM. Further, Bouchut [5] and Aregba-Driollet et al. [1] identified BGK models as a subclass of relaxation systems (RS), which were introduced in [27] and more closely investigated in [17,18]. The linkage of discrete velocity models (DVM) and relaxation systems (RS) was mentioned specifically in the context of LBM for example in [35]. This relationship extends to the discretized versions of DVBE and RS—LBM and relaxation schemes, respectively—and was outlined for mono-dimensional hyperbolic systems by Graille [14].

The importance of a joint treatment of RS and DVBE has been proven when Banda et al. [2] introduced generally applicable tools for *a priori* stability analysis of LBM based on Yong's findings for relaxation systems [43]. These *stability structures* were evaluated more closely by Junk et al. [23], Yong [44], and Rheinländer [37]. Otte et al. [32] applied von Neumann analysis [26,40] for the case of a linear equilibrium. Therein, schemes which are found to be linearly stable also obey the stability structures proposed in [37], which validates the novel approach. In a second study, Otte et al. [33] included stability structures into the derivation of a stable linear lattice Boltzmann collision operator. Caetano et al. [8] recently continued the findings of Graille [14] and delivered elaborate convergence results for a one-dimensional LBM, acting as another indication of the suitability of the DVM and RS linkage for injecting mathematical rigour to the theory of LBM. In DVM, commonly used for LBM simulations, the inclusion of a null velocity is an essential feature, which distinguishes for example $D1Q3$ from $D1Q2$. Nevertheless, previous results, e.g. [8,14] did not extend to discrete velocity sets larger than $D1Q2$ for one-dimensional TEQ and the concatenation of such [14] for the n -dimensional TEQ.

The present work introduces a novel *constructive* approach for the top-down design of discrete velocity Boltzmann equations for a given advection–diffusion equation which appears for example in mathematical models of heat transfer [13] or radiative transport [28]. The formal procedure comprises a perturbation ansatz to obtain a 3×3 RS as a link to a generalized $D1Q3$ DVBE with the corresponding equilibria formally derived from—and pertaining to—the TEQ. Further, the approach includes both velocity sets, $D1Q2$ as well as $D1Q3$, and specifies the necessary extension of the commonly found notes [8,14,34,35,38] on the relation of $D1Q2$ DVBE to the classical 2×2 RS introduced by Liu [27] and Jin et al. [17,18].

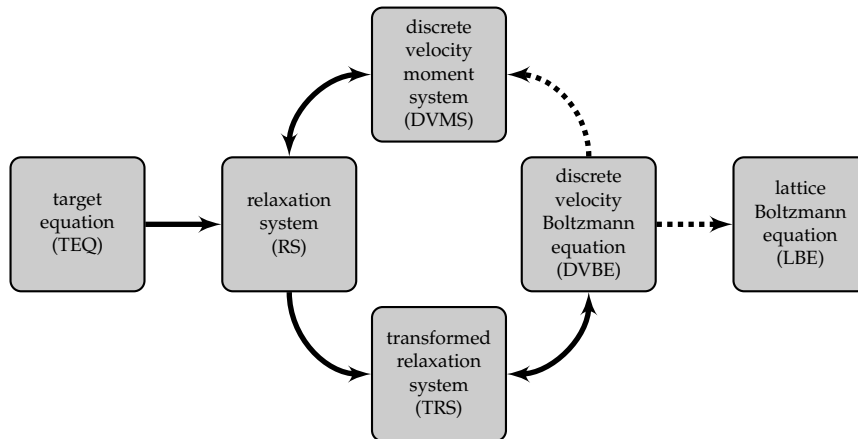


Figure 1: Schematic overview of the constructive approach (from left to right). The steps focused in the present work are labeled with drawn through arrows.

The paper is structured along the proposed design process depicted in Figure 1, starting with the introduction of the herein treated TEQ in Section 2. Based on the TEQ, an RS is constructed in Section 3. Applying spectral decomposition of the hyperbolic part, the RS converges to the TEQ and connects to a generalized DVBE, which is introduced in Section 4 and analyzed in terms of stability structures. A numerical evaluation of the fully discretized lattice Boltzmann equation (LBE) is conducted in Section 5. Concluding the study, specific results are highlighted and currently investigated proceeding topics are exemplarily stated in Section 6.

2. Target equation

The TEQ considered here is a scalar advection–diffusion equation

$$\partial_t \rho + \partial_x F(\rho) - \mu \partial_{xx} \rho = 0, \quad (x, t) \in \mathcal{X} \times \mathcal{I}, \quad (2.1)$$

with initial condition

$$\rho(x, 0) = \rho_0(x), \quad x \in \mathcal{X}. \quad (2.2)$$

For simplicity, we assume that $F: \mathcal{R} \rightarrow \mathbb{R}$ is smooth and linear in the conservative variable $\rho = \rho(x, t) \in \mathcal{R}$, where $x \in \mathcal{X} \subseteq \mathbb{R}$, $t \in \mathcal{I} \subseteq \mathbb{R}^+$, and \mathcal{R} denotes a convex subset of \mathbb{R} . Further, let the diffusion coefficient $\mu > 0$ and $\rho_0 \in L^\infty(\mathcal{X}) \cap L^1(\mathcal{X})$.

Throughout the document it is assumed that \mathcal{X} is periodically embedded in \mathbb{R} and that ρ_0 shares the same periodicity features. Per definition of ρ_0 , F and μ , existence and uniqueness of well-behaved bounded solutions to (2.1) with (2.2) are verified by non-degeneracy and hence uniform parabolicity [7,31].

3. A formal perturbation ansatz for relaxation systems

In [18], RS for hyperbolic problems are proposed and used for subsequent discretization to obtain relaxation schemes which have several numerical advantages. Rheinländer [35] formulates a brief note adding perturbation terms to a hyperbolic conservation law to obtain the 2×2 RS proposed in [18]. The equivalence of this 2×2 RS to a $D1Q2$ DVBE was mentioned for example in [4,35].

As a continuation of the approach in [35], the present work introduces arbitrary scaling by generalization of the perturbation coefficients depending on $\epsilon > 0$, and adds a second perturbation step. Two scalings are included, in particular $\gamma = 1$ corresponds to *hyperbolic* scaling and $\gamma = 2$ denotes *parabolic* scaling. Based on that, $\delta = 2(\gamma - 1)$ is introduced. The terms

hyperbolic and parabolic stem from the TEQ obtained in the perturbation limit ($\epsilon \rightarrow 0$), which is discussed further below.

We start with a scalar conservation law

$$\partial_t \rho + \partial_x F(\rho) = 0, \quad (x, t) \in \mathcal{X} \times \mathcal{I}, \quad (3.1)$$

obtained from neglecting the diffusion term in (2.1). Two subsequent steps are performed, each consisting of the introduction of an artificial variable (AV) and the addition of perturbation terms (AP) including the (stability) constants $\tau, a_1, a_2 > 0$. In particular,

$$\begin{aligned} \text{AV: } \phi = F(\rho) &\Rightarrow \begin{cases} \partial_t \rho + \partial_x \phi = 0 \\ 0 = F(\rho) - \phi \end{cases}, \\ \text{AP: } \epsilon^\gamma \tau \left(\partial_t \phi^\epsilon + \frac{a_1}{\epsilon^\delta} \partial_x \rho^\epsilon \right) = F(\rho^\epsilon) - \phi^\epsilon &\Rightarrow \begin{cases} \partial_t \rho^\epsilon + \partial_x \phi^\epsilon = 0 \\ \partial_t \phi^\epsilon + \frac{a_1}{\epsilon^\delta} \partial_x \rho^\epsilon = -\frac{1}{\epsilon^\gamma \tau} (\phi^\epsilon - F(\rho^\epsilon)) \end{cases}, \\ \text{AV: } \psi^\epsilon = \frac{a_1}{\epsilon^\delta} \rho^\epsilon &\Rightarrow \begin{cases} \partial_t \rho^\epsilon + \partial_x \phi^\epsilon = 0 \\ \partial_t \phi^\epsilon + \partial_x \psi^\epsilon = -\frac{1}{\epsilon^\gamma \tau} (\phi^\epsilon - F(\rho^\epsilon)) \\ 0 = \frac{a_1}{\epsilon^\delta} \rho^\epsilon - \psi^\epsilon \end{cases}, \\ \text{AP: } \epsilon^\gamma \tau \left(\partial_t \psi^{\epsilon\epsilon} + \frac{a_2}{\epsilon^\delta} \partial_x \phi^{\epsilon\epsilon} \right) = \frac{a_1}{\epsilon^\delta} \rho^{\epsilon\epsilon} - \psi^{\epsilon\epsilon} &\Rightarrow \begin{cases} \partial_t \rho^{\epsilon\epsilon} + \partial_x \phi^{\epsilon\epsilon} = 0 \\ \partial_t \phi^{\epsilon\epsilon} + \partial_x \psi^{\epsilon\epsilon} = -\frac{1}{\epsilon^\gamma \tau} (\phi^{\epsilon\epsilon} - F(\rho^{\epsilon\epsilon})) \\ \partial_t \psi^{\epsilon\epsilon} + \frac{a_2}{\epsilon^\delta} \partial_x \phi^{\epsilon\epsilon} = -\frac{1}{\epsilon^\gamma \tau} (\psi^{\epsilon\epsilon} - \frac{a_1}{\epsilon^\delta} \rho^{\epsilon\epsilon}) \end{cases}. \end{aligned} \quad (3.2)$$

Fixing $\tau = 1$, system (3.2) resembles an approximation to hyperbolic conservation laws, since for $\gamma = 1$ the 2×2 RS in [18] is obtained, whereas $\gamma = 2$ yields the *diffusive* 2×2 RS which was proposed in [17] and further analyzed in [4]. For system (3.2), the limits ($\epsilon \rightarrow 0$) to (3.1) or (2.1), for $\gamma = 1$ or $\gamma = 2$, respectively, were proven in [4,18].

Formally, upon condition that $\rho^{\epsilon\epsilon}, \phi^{\epsilon\epsilon}$, and $\psi^{\epsilon\epsilon}$ are sufficiently smooth, we can transform (3.3) to an equivalent closed equation in $\rho^{\epsilon\epsilon}$ relating to (2.1) via added perturbation terms. The assumption on smoothness is necessary for the generalization of Schwarz's theorem to enable free permutation of variables in higher order partial derivatives. Let (I), (II) and (III) denote the first, second and third equation of (3.3), respectively. Solving (III) for $\psi^{\epsilon\epsilon}$, and inserting it into (II) yields

$$\partial_t \phi^{\epsilon\epsilon} - \epsilon^\gamma \tau \partial_{tx} \psi^{\epsilon\epsilon} - \epsilon^\gamma \tau \frac{a_2}{\epsilon^\delta} \partial_{xx} \phi^{\epsilon\epsilon} + \frac{a_1}{\epsilon^\delta} \partial \rho^{\epsilon\epsilon} = \frac{1}{\epsilon^\gamma \tau} (\phi^{\epsilon\epsilon} - F(\rho^{\epsilon\epsilon})). \quad (3.4)$$

We can solve ∂_t (II) for $\partial_{xt} \psi^{\epsilon\epsilon} = \partial_{tx} \psi^{\epsilon\epsilon}$ and substitute it in (3.4), which gives

$$2\partial_t \phi^{\epsilon\epsilon} - \partial_t F(\rho^{\epsilon\epsilon}) + \epsilon^\gamma \tau \partial_{tt} \phi^{\epsilon\epsilon} - \epsilon^\gamma \tau \frac{a_2}{\epsilon^\delta} \partial_{xx} \phi^{\epsilon\epsilon} + \frac{a_1}{\epsilon^\delta} \partial \rho^{\epsilon\epsilon} = \frac{1}{\epsilon^\gamma \tau} (\phi^{\epsilon\epsilon} - F(\rho^{\epsilon\epsilon})). \quad (3.5)$$

Solving (3.5) for $\phi^{\epsilon\epsilon}$ and injecting it into (I) results (after reordering terms) in

$$\partial_t \rho^{\epsilon\epsilon} + \partial_x F(\rho^{\epsilon\epsilon}) - \epsilon^\gamma \tau \frac{a_1}{\epsilon^\delta} \partial_{xx} \rho^{\epsilon\epsilon} = \epsilon^\gamma \tau \left\{ -\partial_{tx} F(\rho^{\epsilon\epsilon}) + \partial_{tx} \phi^{\epsilon\epsilon} + \epsilon^\gamma \tau \partial_{ttt} \phi^{\epsilon\epsilon} - \epsilon^\gamma \tau \frac{a_2}{\epsilon^\delta} \partial_{xxx} \phi^{\epsilon\epsilon} \right\}. \quad (3.6)$$

From ∂_{xx} (I), ∂_t (I), and ∂_{tt} (I) we get expressions in $\rho^{\epsilon\epsilon}$ for the remaining $\phi^{\epsilon\epsilon}$ -derivatives on the right-hand side of (3.6). Finally, this forms a closed equation in the conservative variable,

$$\partial_t \rho^{\epsilon\epsilon} + \partial_x F(\rho^{\epsilon\epsilon}) - \epsilon^{2-\gamma} a_1 \tau \partial_{xx} \rho^{\epsilon\epsilon} = \epsilon^\gamma \tau \left\{ -\partial_{xt} F(\rho^{\epsilon\epsilon}) - 2\partial_{tt} \rho^{\epsilon\epsilon} - \epsilon^\gamma \tau \partial_{ttt} \rho^{\epsilon\epsilon} + \epsilon^{2-\gamma} a_2 \tau \partial_{xxx} \rho^{\epsilon\epsilon} \right\}. \quad (3.7)$$

In the formal limit $\epsilon \rightarrow 0$, the perturbation terms on the right-hand side of (3.7) vanish due to their prefactor ϵ^γ . Note that, in the limit, the presence of the diffusion term on the left-hand side

depends on γ . Hence, the scaling completely determines the diffusion effects. In the case of $\gamma = 2$, μ is recovered in the formal limit through $a_1\tau$.

Remark 3.1. Based on equation (3.7) we infer that, the diffusion coefficient in the parabolic limit of the RS (3.3) can be altered with the modification of τ . In case of $\gamma = 1$ however, this alteration does not interfere with the formal limit to the hyperbolic conservation law itself, since for ϵ small enough, the constant τ merely acts as a prefactor for the $\mathcal{O}(\epsilon)$ diffusion term.

Remark 3.2. A convergence proof of the limit of a diffusive 2×2 RS towards (2.1) with $F \equiv 0$, starting at the equivalent closed equation with a splitting of the initial condition (2.2), is given in [35]. In the present work we omit such an analysis and solely remark that the extension thereof can be obtained from including the third order derivatives of (3.7). For convergence to the TEQ we continue with transforming (3.3) to enable the usage of more general results from [7].

The constructed 3×3 RS (3.3) can be written in matrix notation as

$$\partial_t \begin{pmatrix} \rho^{\epsilon\epsilon} \\ \phi^{\epsilon\epsilon} \\ \psi^{\epsilon\epsilon} \end{pmatrix} + \underbrace{\begin{bmatrix} 0 & 1 & 0 \\ 0 & 0 & 1 \\ 0 & \frac{a_2}{\epsilon^\delta} & 0 \end{bmatrix}}_{=: A} \partial_x \begin{pmatrix} \rho^{\epsilon\epsilon} \\ \phi^{\epsilon\epsilon} \\ \psi^{\epsilon\epsilon} \end{pmatrix} = -\frac{1}{\epsilon^\gamma \tau} \begin{pmatrix} 0 \\ \phi^{\epsilon\epsilon} - F(\rho^{\epsilon\epsilon}) \\ \psi^{\epsilon\epsilon} - \frac{a_1}{\epsilon^\delta} \rho^{\epsilon\epsilon} \end{pmatrix}. \quad (3.8)$$

Via the spectral decomposition

$$A = DA^d D^{-1} = \begin{bmatrix} 1 & 1 & 1 \\ -\sqrt{\chi} & 0 & \sqrt{\chi} \\ \chi & 0 & \chi \end{bmatrix} \begin{bmatrix} -\sqrt{\chi} & 0 & 0 \\ 0 & 0 & 0 \\ 0 & 0 & \sqrt{\chi} \end{bmatrix} \begin{bmatrix} 0 & -\frac{1}{2\sqrt{\chi}} & \frac{1}{2\chi} \\ 1 & 0 & -\frac{1}{\chi} \\ 0 & \frac{1}{2\sqrt{\chi}} & \frac{1}{2\chi} \end{bmatrix}, \quad (3.9)$$

where

$$\chi := \frac{a_2}{\epsilon^\delta},$$

we can rewrite system (3.8) by a change of variables

$$\begin{pmatrix} u \\ v \\ w \end{pmatrix} := D^{-1} \begin{pmatrix} \rho^{\epsilon\epsilon} \\ \phi^{\epsilon\epsilon} \\ \psi^{\epsilon\epsilon} \end{pmatrix} \Leftrightarrow \begin{pmatrix} \rho^{\epsilon\epsilon} \\ \phi^{\epsilon\epsilon} \\ \psi^{\epsilon\epsilon} \end{pmatrix} = D \begin{pmatrix} u \\ v \\ w \end{pmatrix} = \begin{pmatrix} u + v + w \\ \frac{1}{\sqrt{\chi}}(-u + w) \\ \frac{1}{\chi}(u + w) \end{pmatrix},$$

to obtain a *transformed relaxation system* (TRS)

$$\partial_t \begin{pmatrix} u \\ v \\ w \end{pmatrix} + A^d \partial_x \begin{pmatrix} u \\ v \\ w \end{pmatrix} = -\frac{1}{\epsilon^\gamma \tau} \begin{pmatrix} u - \frac{a_1}{2a_2}(u + v + w) + \frac{1}{2\sqrt{\chi}}F(u + v + w) \\ v - (1 - \frac{a_1}{a_2})(u + v + w) \\ w - \frac{a_1}{2a_2}(u + v + w) - \frac{1}{2\sqrt{\chi}}F(u + v + w) \end{pmatrix}. \quad (3.10)$$

Bouchut [6] summarized stability conditions for relaxation systems and compared relations between the available approaches to prove the correct limiting behaviour for $\epsilon \rightarrow 0$. The notes in [6] comprise observations by Bouchut et al. [7] for frameworking relaxation systems to obtain possibly degenerate advection–diffusion equations. Convergence is thereafter given if specific assumptions are satisfied. Based on that, we use the results from [7] to prove the convergence of (3.10) towards (2.1) in the limit $\epsilon \rightarrow 0$. We define a function

$$G : [0, 1] \times \mathbb{R} \rightarrow \mathbb{R}^3, (\epsilon, \alpha) \mapsto \begin{pmatrix} \frac{a_1}{2a_2}\alpha - \frac{1}{2\sqrt{\chi}}F(\alpha) \\ (1 - \frac{a_1}{a_2})\alpha \\ \frac{a_1}{2a_2}\alpha + \frac{1}{2\sqrt{\chi}}F(\alpha) \end{pmatrix}, \quad (3.11)$$

and denote it as *generalized Maxwellian*. Further, let $U = \{\alpha \in \mathbb{R} : |\alpha| \leq \|\rho_0\|_\infty\}$ and $F(0) = 0$.

Corollary 3.1. Let $\tau = 1$. Equip the TRS (3.10) with initial data $(u, v, w)^T = G(\epsilon, \rho_0)$ and specify the stability constants in the above proposed perturbation ansatz such that $a_1 = \mu$ and

$$a_2 \geq a_1 \quad \wedge \quad \frac{a_1}{\sqrt{\epsilon^\delta a_2}} \geq |F'(\rho)|. \quad (3.12)$$

Then

$$\lim_{\epsilon \searrow 0} \rho^{\epsilon\epsilon} = \rho^* \in C(\mathcal{I}; L^1_{loc}(\mathcal{X})) \cap L^\infty(\mathcal{X} \times \mathcal{I})$$

is the unique entropy solution to the TEQ (2.1) with initial data (2.2).

Proof. The constraints on G given in [7],

$$\begin{aligned} (M_1) \quad & \sum_{i=1}^3 G_i(\epsilon, \alpha) = \alpha && \forall \epsilon \in (0, 1] \quad \forall \alpha \in U, \\ (M_2) \quad & \sum_{i=1}^3 A^d G_i(\epsilon, \alpha) = F(\alpha) && \forall \epsilon \in (0, 1] \quad \forall \alpha \in U, \\ (M_3) \quad & \sum_{i=1}^3 (\sqrt{\epsilon^\delta} A_{i,i})^2 G_i(0, \alpha) = \mu \alpha && \forall \alpha \in U, \\ (M_4) \quad & \lim_{\epsilon \searrow 0} G_i(\epsilon, \alpha) = G_i(0, \alpha) && \text{uniformly for } \alpha \in U, \end{aligned}$$

are verified. By construction, $G(\epsilon, 0) = 0 \quad \forall \epsilon \in [0, 1]$ follows from $F(0) = 0$, and $G_i(\epsilon, \cdot)$ is nondecreasing in U for $i = 1, 2, 3$ and $\epsilon \in (0, 1]$ due to condition (3.12). Hence, the claim follows from [7, Theorem 3.1 and Theorem 4.1]. \square

4. The link to discrete velocity Boltzmann models

The following investigations link the approach given above to a DVBE which under subsequent discretization leads to an LBM as commonly proposed in the community [25,29]. Therefor, we construct a DVBE with generalized ingredients to match the generality of the TRS obtained in Section 3, and use the equivalence of both systems to prove the convergence of the DVBE towards the TEQ.

Roughly speaking, DVBE are obtained by reducing the velocity space \mathcal{V} of the Boltzmann BGK equation

$$\partial_t f + \mathbf{v} \cdot \nabla_{\mathbf{x}} f = \Omega(f) = -\omega(f - f^{\text{eq}}) \quad (4.1)$$

to a finite set $\mathcal{C} = \{\mathbf{c}_i\}_{i=0,1,\dots,q-1} \subset \mathcal{V}$, abbreviated with $DdQq$. In (4.1), the (equilibrium) particle distribution function $f^{(\text{eq})} : \mathcal{X} \times \mathcal{V} \times \mathcal{I} \ni (\mathbf{x}, \boldsymbol{\xi}, t) \mapsto f^{(\text{eq})}(\mathbf{x}, \boldsymbol{\xi}, t) \in \mathbb{R}_0^+$ resembles the density of mass in $\mathcal{X} \subseteq \mathbb{R}^d$, $\mathcal{V} \subseteq \mathbb{R}^d$ and $\mathcal{I} \subseteq \mathbb{R}_0^+$ (at equilibrium), and ω denotes the relaxation frequency. The resulting DVBE with the BGK collision operator, equipped with the general scaling introduced above, then reads

$$\epsilon^\gamma \partial_t \mathbf{f}_i + \epsilon \mathbf{c}_i \cdot \nabla_{\mathbf{x}} \mathbf{f}_i = J_i(f) = -\omega [f_i - f_i^{\text{eq}}], \quad i = 0, \dots, q-1, \quad (4.2)$$

where $f_i(x, t)$ denote discrete velocity distribution functions (populations) with corresponding equilibria $f_i^{\text{eq}} = E_i(f)$. Additionally, via a weight function $w : \mathcal{C} \rightarrow \mathbb{R}$, each $\mathbf{c}_i \in \mathcal{C}$ is assigned a weight $w_i = w(\mathbf{c}_i)$.

In (4.2) and in the following, we adopt the notation introduced by Rheinländer [35]. That is, maps contained in the space of functions over \mathcal{C} , here abbreviated by $\mathcal{C}^* := \mathcal{F}(\mathcal{C})$, as well as their vector representations are denoted by the same symbol, e.g. $w = (w_0, \dots, w_{q-1})^T$. The (by construction) linearly independent component maps $\mathbf{s}_j = ((c_0)_j, \dots, (c_{q-1})_j)^T$, $j = 1, \dots, d$, can be completed with linearly independent vectors $\tilde{\mathbf{s}}_k$, $k = d+1, \dots, q$, to a basis such that $\mathcal{C}^* =$

$\text{span}\{s_1, \dots, s_d, \tilde{s}_{d+1}, \dots, \tilde{s}_q\} \cong \mathbb{R}^q$. Typically, polynomials in s_j are used for the basis completion [10]. Further, $\langle \cdot, \cdot \rangle$ defines the scalar product on C^* , whereas no product sign between two maps in C^* refers to component-wise multiplication.

To include the velocity set $D1Q2$, let the weights depend on $\theta > 0$, where $\theta \rightarrow 1$ transforms $D1Q3$ into $D1Q2$ [35]. Additionally, we generalize the velocity model with a variable speed λ . For $\mathcal{C} = \{-\lambda, 0, \lambda\}$, the velocity component map reads $\mathbf{s} = s_1 = (-\lambda, 0, \lambda)^T$ with corresponding weights $\mathbf{w} = w(\mathbf{s}) = (\frac{1}{2\theta}, \frac{\theta-1}{\theta}, \frac{1}{2\theta})$. We obtain $C^* = \text{span}\{1, \mathbf{s}, \mathbf{s}^2\}$, and more specifically

$$\mathbf{s}^n = \begin{cases} 1, & \text{if } n = 0, \\ \lambda^{n-1} \mathbf{s}, & \text{if } n \text{ odd,} \\ \lambda^{n-2} \mathbf{s}^2, & \text{if } n \text{ even.} \end{cases}$$

The here required structure relations for $D1Q3$ are given by

$$\langle 1, \mathbf{w} \rangle = 1, \quad \langle \mathbf{s}, \mathbf{w} \rangle = 0, \quad \langle \mathbf{s}^2, \mathbf{w} \rangle = \frac{\lambda^2}{\theta}, \quad \langle \mathbf{s}^3, \mathbf{w} \rangle = 0. \quad (4.3)$$

Respecting the inverse proportionality between the velocity and the scaling parameter ϵ , we define three raw moments [10], i.e.

$$m_0 = \langle 1, f \rangle, \quad m_1 = \frac{1}{\epsilon^{\gamma-1}} \langle \mathbf{s}, f \rangle, \quad m_2 = \frac{1}{\epsilon^{2(\gamma-1)}} \langle \mathbf{s}^2, f \rangle. \quad (4.4)$$

We assume that only m_0 requires conservation, identifying it with the conservative variable ρ in (2.1). The equilibrium populations $E(f)$ can be expressed via the equilibrium operator $\varepsilon(m_0; \cdot) \in C^*$, depending solely on conserved moments which are generated by the *collisional invariant* monomials, here $1 = \mathbf{s}^0$. The relations (4.3) can be used in an algebraic argument, which is based on the injection of $E(f)$ into the TEQ [35] and extended by removal of scaling dependent terms. The solution of the resulting linear system leads to the determination of

$$E(f) = \varepsilon(m_0; \mathbf{s}) = m_0 \mathbf{w} + \epsilon^{\gamma-1} \frac{\theta}{\lambda^2} F(m_0) \mathbf{w} \mathbf{s}. \quad (4.5)$$

Inserting (4.5), with \mathcal{C} , m_0 , \mathbf{s} and \mathbf{w} into (4.2), plus subsequent multiplication with $\epsilon^{-\gamma}$, results in a $D1Q3$ DVBE

$$\partial_t \begin{pmatrix} f_0 \\ f_1 \\ f_2 \end{pmatrix} + \begin{bmatrix} -\frac{\lambda}{\epsilon^{\gamma-1}} & 0 & 0 \\ 0 & 0 & 0 \\ 0 & 0 & \frac{\lambda}{\epsilon^{\gamma-1}} \end{bmatrix} \partial_x \begin{pmatrix} f_0 \\ f_1 \\ f_2 \end{pmatrix} = -\frac{\omega}{\epsilon^\gamma} \begin{pmatrix} f_0 - \frac{1}{2\theta} (f_0 + f_1 + f_2) + \frac{\epsilon^{\gamma-1}}{2\lambda} F(f_0 + f_1 + f_2) \\ f_1 - \frac{\theta-1}{\theta} (f_0 + f_1 + f_2) \\ f_2 - \frac{1}{2\theta} (f_0 + f_1 + f_2) - \frac{\epsilon^{\gamma-1}}{2\lambda} F(f_0 + f_1 + f_2) \end{pmatrix}. \quad (4.6)$$

Theorem 4.1. *Let $\omega = 1$. The $D1Q3$ DVBE (4.6) with initial data $f(x, 0) = \varepsilon(\rho_0; \mathbf{s})$ converges in $C(\mathcal{I}; L^1_{loc}(\mathcal{X}))$ to the bounded unique entropy solution of (2.1) with initial condition (2.2).*

Proof. Comparing (4.6) to (3.10), equivalence of the $D1Q3$ DVBE and the 3×3 TRS is obtained via identifying the stability parameters

$$\tau := \frac{1}{\omega}, \quad a_1 := \frac{\lambda^2}{\theta}, \quad a_2 := \lambda^2. \quad (4.7)$$

Thus, with $\varepsilon(\cdot; \mathbf{s}) \equiv G(\epsilon, \cdot)$ and $\tau = 1$, convergence to the TEQ follows from Corollary 3.1. \square

Remark 4.1. *The parameter setting (4.7) additionally generates equivalence of the initially constructed RS (3.3) and the discrete velocity moment system (DVMS), obtained from taking the moments*

$$\langle 1, \cdot \rangle, \quad \frac{1}{\epsilon^{\gamma-1}} \langle \mathbf{s}, \cdot \rangle, \quad \frac{1}{\epsilon^{2(\gamma-1)}} \langle \mathbf{s}^2, \cdot \rangle$$

of (4.6). Hence, this moment summation reflects the reverse action of the spectral decomposition in (3.9).

Rheinländer [37] extended the stability structures proposed by Banda et al. [2] for DVBE, to a self-contained *a priori* stability notion for LBE (i.e. the fully discretized version of the DVBE). The statements on *pre-stability* in [37] are still valid to obtain structural stability also for the DVBE. However, it is essential to mention that the following derivations are based on the linearity of F , which allows to express the collision operator as a linear map in matrix form by simply taking the Jacobian. In case of a non-linear collision operator, Banda et al. [2] formulated corresponding results for the linearized operator around an equilibrium state \mathbf{f}^* .

Definition 4.1. Rheinländer [37]: The collision operator J in (4.2) admits a pre-stability structure, if there exists $H \in \text{GL}_q(\mathbb{R})$ and $\mathbf{p} = (p_1, \dots, p_q)^T$, $\mathbf{r} = (r_1, \dots, r_q)^T \in \mathbb{R}^q$ such that

$$\begin{cases} H J_{\mathbf{f}} = -\text{diag}(\mathbf{p}) H, \\ H^T H = \text{diag}(\mathbf{r}). \end{cases}$$

Corollary 4.1. The D1Q3 collision operator

$$J^{D1Q3} = -\frac{\omega}{\epsilon^\gamma} [\mathbf{f} - E(\mathbf{f})],$$

defined in (4.6), admits a pre-stability structure, if

$$\theta > 1 \quad \wedge \quad \frac{\lambda}{\theta \epsilon^{\gamma-1}} > |F'|. \quad (4.8)$$

Proof. The Jacobian of the collision operator in (4.6) reads

$$J_{\mathbf{f}}^{D1Q3}(\mathbf{f}) = -\frac{\omega}{\epsilon^\gamma} \left(I_3 - \underbrace{\begin{bmatrix} \frac{1}{2\theta} - \frac{\epsilon^{\gamma-1}}{2\lambda} F' & \frac{1}{2\theta} - \frac{\epsilon^{\gamma-1}}{2\lambda} F' & \frac{1}{2\theta} - \frac{\epsilon^{\gamma-1}}{2\lambda} F' \\ \frac{\theta-1}{\theta} & \frac{\theta-1}{\theta} & \frac{\theta-1}{\theta} \\ \frac{1}{2\theta} + \frac{\epsilon^{\gamma-1}}{2\lambda} F' & \frac{1}{2\theta} + \frac{\epsilon^{\gamma-1}}{2\lambda} F' & \frac{1}{2\theta} + \frac{\epsilon^{\gamma-1}}{2\lambda} F' \end{bmatrix}}_{=E_{\mathbf{f}}(\mathbf{f})} \right).$$

Each column of $E_{\mathbf{f}}$ sums up to 1. Hence, the Jacobian is a projector, i.e.

$$[E_{\mathbf{f}}(\mathbf{f})]^2 = E_{\mathbf{f}}(\mathbf{f}).$$

Note that this is already fulfilled for the generalized Maxwellian (3.11). Henceforth,

$$K = \text{diag} \left(\frac{1}{2\theta} - \frac{\epsilon^{\gamma-1}}{2\lambda} F', \frac{\theta-1}{\theta}, \frac{1}{2\theta} + \frac{\epsilon^{\gamma-1}}{2\lambda} F' \right)$$

is a unique symmetrizer for $E_{\mathbf{f}}$. Condition (4.8) implies that K is positive definite. The results in [37, Theorem 6, Proposition 13] specify the existence and definition of H , \mathbf{p} and \mathbf{r} , and thus complete the proof. \square

Remark 4.2. The inequalities (3.12) in Corollary 3.1 for the TRS are precisely the stability conditions (4.8) in Theorem 4.1 for the DVBE, except of the possible equality in (3.12). This observation fits to Rheinländer's [37] statement that the existence of a stability structure is only a sufficient condition for stability.

Remark 4.3. The typical space and explicit Euler in time discretization for LBM leads to a stability structure under an additional condition on the final relaxation frequency appearing in the LBE [37]: $\omega_{\Delta x} \in [0, 2]$, where Δx is the space discretization parameter related to ϵ . An example with specific parameter choices is given in Section 5 and verifies the observations in [35,37]. Further, a numerical comparison between LBM with the herein given equilibrium population and LBM with an extended Navier–Stokes equilibrium is given in [9]. From a formal point of view, the inclusion of extended equilibria into the current framework would require extended perturbation terms for the steps AP in the proposed ansatz (Section 3), effectuating additional terms on the right-hand side of (3.7).

5. Lattice Boltzmann equation—numerical examples

The generality of the herein presented ansatz is reflected in the fact that by varying model parameters in the constructed DVBE, we can reach either an advection–diffusion equation, a diffusion equation, or a hyperbolic conservation law. The following numerical tests investigate the applicability of the stability constraints derived above and suggest approximation orders to the TEQ. An in detail analysis of accuracy and consistency in each step from TEQ to LBE is not carried out, though subject to follow-up research. Nevertheless, for the sake of completeness we briefly recall the classical discretization process.

Given the DVBE (4.2), an LBE can be obtained by complete discretization. As a starting point, we integrate (4.2) for $\mathbf{c}_i \in \mathcal{C}$ along the characteristic [35]

$$(\hat{\mathbf{x}}(\eta), \hat{t}(\eta)) = (\mathbf{x} + \epsilon^{1-\gamma} \mathbf{c}_i \eta, t + \eta).$$

Integrating from 0 to ϵ^γ and identifying the total derivative of f_i with respect to η leads to exact integration on the left-hand side, i.e.

$$f_i(\hat{\mathbf{x}}(\epsilon^\gamma), \hat{t}(\epsilon^\gamma)) - f_i(\mathbf{x}, t) = \frac{1}{\epsilon^\gamma} \int_0^{\epsilon^\gamma} J_i(\hat{\mathbf{x}}, \hat{t}) d\eta. \quad (5.1)$$

A basic Euler explicit rule approximates the integral on the right-hand side of (5.1) with its left integration bound, hence

$$f_i(\mathbf{x} + \epsilon \mathbf{c}_i, t + \epsilon) - f_i(\mathbf{x}, t) = -\omega [f_i(\mathbf{x}, t) - f_i^{\text{eq}}(\mathbf{x}, t)] + \mathcal{O}(\epsilon^\gamma).$$

Via neglecting the γ -th order terms and introducing $\Delta t = \Delta x^\gamma$, where $\Delta x = \epsilon$, we obtain the fully discrete LBE

$$f_i(\mathbf{x} + \Delta x \mathbf{c}_i, t + \Delta t) - f_i(\mathbf{x}, t) = -\omega_{\Delta x} [f_i(\mathbf{x}, t) - f_i^{\text{eq}}(\mathbf{x}, t)], \quad (5.2)$$

which operates on a uniform spatial lattice $\mathcal{X}_{\Delta x}$. The lattice is assumed to be invariant under discrete velocity translation, i.e. $\forall \mathbf{x} \in \mathcal{X}_{\Delta x} : \mathbf{x} + \Delta x \mathbf{c}_i \in \mathcal{X}_{\Delta x}$ for $i = 0, 1, \dots, q - 1$. For in detail derivations of several, possibly higher order discretizations of the DVBE, we refer the reader to He et al. [16], Junk et al. [20], Rheinländer [35], Ubertini et al. [41], Krause [24], Dellar [11], and Krüger et al. [25].

Remark 5.1. *The pathway from the DVBE to the LBE is not focused in the present work. The topic itself however is controversial, since the assignment $\epsilon^\gamma = \Delta x^\gamma = \Delta t$ amalgamates the relaxation limit and the mesh dependence. The LBE derivation is based on a top-down discretization of the DVBE, which in turn limits towards the TEQ when $\epsilon \rightarrow 0$. Hence, accuracy orders are typically expressed with respect to the DVBE. A sublime discussion on DVBE discretization orders is provided by Ubertini et al. [41]. In contrast, consistency results for the LBE with respect to the TEQ are often based on asymptotic analysis [20,22].*

For the following examples, the accuracy of the D1Q3 LBE with respect to the TEQ is assessed numerically by a time-dependent L_2 -error [25], as well as a global error obtained from averaging over fixed physical points in time, respectively

$$\text{err}_{L_2}(t_m) = \sqrt{\frac{\sum_{n=0}^N |m_0(x_n, t_m) - \rho^*(x_n, t_m)|^2}{\sum_{n=0}^N |\rho^*(x_n, t_m)|^2}}, \quad \overline{\text{err}} = \frac{1}{M} \sum_{m=1}^M \text{err}_{L_2}(t_m), \quad (5.3)$$

where $x_n = n\Delta x$ and $t_m = m\Delta t$.

(a) Linear advection–diffusion equation

Consider the initial value problem

$$\begin{cases} \partial_t \rho + u \partial_x \rho - \mu \partial_{xx} \rho = 0, & (x, t) \in (-1, 1) \times (0, \infty), \\ \rho_0(x) \equiv \rho(x, 0) = \sin(\pi x), & x \in (-1, 1), \end{cases} \quad (5.4)$$

with periodic boundaries. According to Mojtabi et al. [30], the analytical solution to (5.4) is

$$\rho^*(x, t) = \sin(\pi(x - ut)) \exp(-\mu\pi^2 t). \quad (5.5)$$

The model is uniquely defined by the non-dimensional Peclet number $Pe = uL/\mu$, where $u \in \mathbb{R}$ is the advection velocity, $L = 2$ is the domain size and $\mu > 0$ denotes the diffusion coefficient.

Table 1 summarizes the parameter choices for the conducted simulations to approximate the solution of (5.4) with the $D1Q3$ LBE. The mathematical model parameters are chosen as $\lambda = 1$ and $\theta = 3$, whereas the physical advection velocity is set to $u = 10$. The time evolution of the approximated conservative variable is exemplarily visualized in Figure 3a. The asymptotic analysis executed in [22] predicts theoretical second order convergence in space for $D1Q2$ and $D1Q3$ LBM with respect to advection–diffusion–reaction equations. Further, it can be deduced that the diffusion coefficient is recovered by the LBM as

$$\mu = \frac{\Delta t}{3} \left(\frac{1}{\omega_{\Delta x}} - \frac{1}{2} \right).$$

If not stated otherwise, the terminal time t_M for \overline{err} in (5.3) is determined such that for each choice of Pe in Table 1, the initial pulse ρ_0 is diffused to an amplitude of $\max_n |\rho(x_n, t_M)| \leq 0.01$. Individual error values are summarized in Table 2. The numerical test cases approve the second order accuracy with respect to the TEQ in the present setting, see Figure 3b and Table 2, where the respective experimental order of convergence \overline{EOC} was calculated from averaging convergence speeds obtained for two subsequent resolutions, respectively [15]. Concerning stability, the above derivations can be used to obtain a sufficient condition on the stability of the scheme. Dependent on the advection velocity $F' \equiv u$, we deduce from $\epsilon = \Delta x$, $\theta = 3$, $\lambda = 1$, and $\gamma = 2$ that

$$\Delta x < \frac{1}{3|u|}. \quad (5.6)$$

However, the quality of the bound is dependent on $\omega_{\Delta x}$. For our setting, with $u = 10$, we obtain a maximum mesh size of $\Delta x \leq 0.0\bar{3}$. Since instabilities appear after $t > 0.3$ for a parameter combination of $\omega_{\Delta x} = 1.8$ and $\Delta x = 0.04 > 0.0\bar{3}$, Table 2 suggests that along $\omega_{\Delta x} \rightarrow 2$ the bound sharpens and reaches the analytical region depicted in Figure 2. This observation matches the results in [37,39] obtained with spectral radius calculation of the evolution operator of the LBE (5.2).

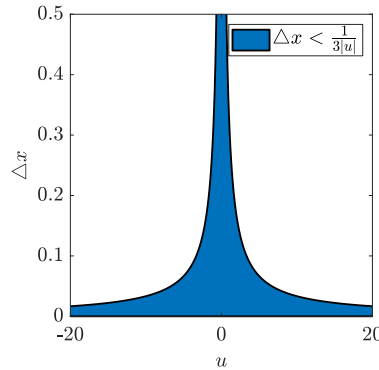


Figure 2: Structural stability bound (5.6) for the $D1Q3$ LBE advection–diffusion approximation.

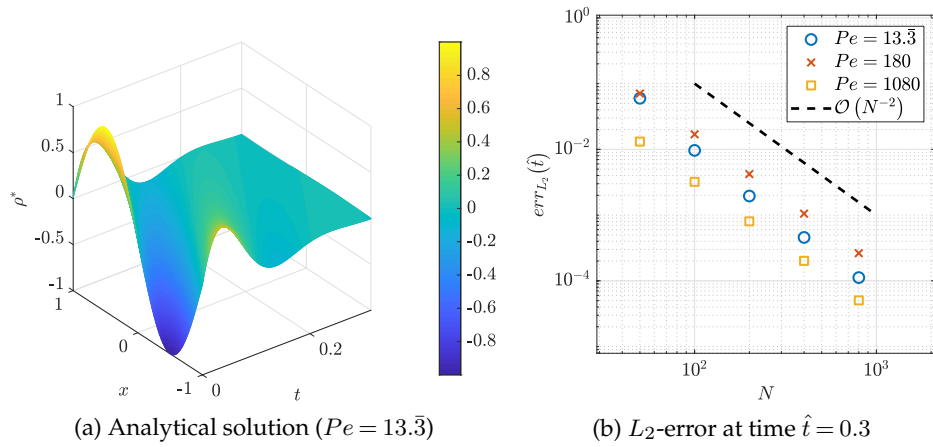


Figure 3: (a) Exemplary analytical solution (5.5) for $Pe = 13.\bar{3}$ plotted until terminal time t_M . (b) L_2 -error at time $\hat{t} = 0.3$ for linear advection–diffusion tests with parameters from Table 1.

Table 1: Summary of parabolically scaled LBM discretization parameters (\cdot_L denotes lattice units). Note that $\mu = \mu_L$.

parabolic scaling $\gamma = 2$				$\mu = 1.5$ $Pe = 13.\bar{3}$	$\mu = 0.\bar{1}$ $Pe = 180$	$\mu = 0.0\bar{1}85$ $Pe = 1080$
N	u_L	Δx	Δt	$\omega_{\Delta x}$		
50	4×10^{-1}	4×10^{-2}	1.6×10^{-3}	0.2	1.2	1.8
100	2×10^{-1}	2×10^{-2}	4×10^{-4}	0.2	1.2	1.8
200	1×10^{-1}	1×10^{-2}	1×10^{-4}	0.2	1.2	1.8
400	5×10^{-2}	5×10^{-3}	2.5×10^{-5}	0.2	1.2	1.8
800	2.5×10^{-2}	2.5×10^{-3}	6.25×10^{-6}	0.2	1.2	1.8

Table 2: Numerical errors for parabolically scaled LBM to approximate the advection–diffusion equation (5.4) measured in terms of global error \overline{err} until terminal time t_M , local in time L_2 -error $err_{L_2}(\hat{t})$ at $\hat{t} = 0.3$, and experimental order of convergence \overline{EOC} .

N	$Pe = 13.\bar{3}$		$Pe = 180$		$Pe = 1080$	
	$err_{L_2}(\hat{t})$	\overline{err}	$err_{L_2}(\hat{t})$	\overline{err}	$err_{L_2}(\hat{t})$	\overline{err}
50	0.05989428	0.09943222	0.07072684	0.11399244	0.01314406	—
100	0.00964851	0.02481457	0.01695887	0.01882449	0.00320808	0.01888899
200	0.00195161	0.00583256	0.00421151	0.00431378	0.00080292	0.00432645
400	0.00045732	0.00142989	0.00105309	0.00105990	0.00020130	0.00105915
800	0.00011205	0.00035539	0.00026353	0.00026311	0.00005042	0.00026356
\overline{EOC}	2.2655	2.0320	2.0170	2.1898	2.0065	2.0544

(b) Diffusion equation

Under the assumption that $u = 0$ in (5.4), we obtain a diffusion equation as TEQ. The analytical solution is similarly given by (5.5) with $u = 0$. The nulled out advection velocity leads formally to $Pe = 0$. Hence, the numerical results are obtained from parameters in Table 1, where additionally $u_L = 0$. The analytical solution is exemplarily visualized in Figure 4a.

The numerical tests suggest consistency of second order with respect to the TEQ (Table 3 and Figure 4b) and thus are agreement with Weiss' [42] investigations for the Goldstein–Taylor model (a formal equivalent to a $D1Q2$ DVBE).

In contrast to the results for a non-zero advection velocity, all of the simulations conducted for the diffusion equation as TEQ are stable. The increased stability is reasonable in view of the theoretical prediction derived above. More precisely, from (5.6), we may infer that $\Delta x < \infty$. Hence, structural stability is given unconditionally for $\omega_{\Delta x} \in (0, 2)$.

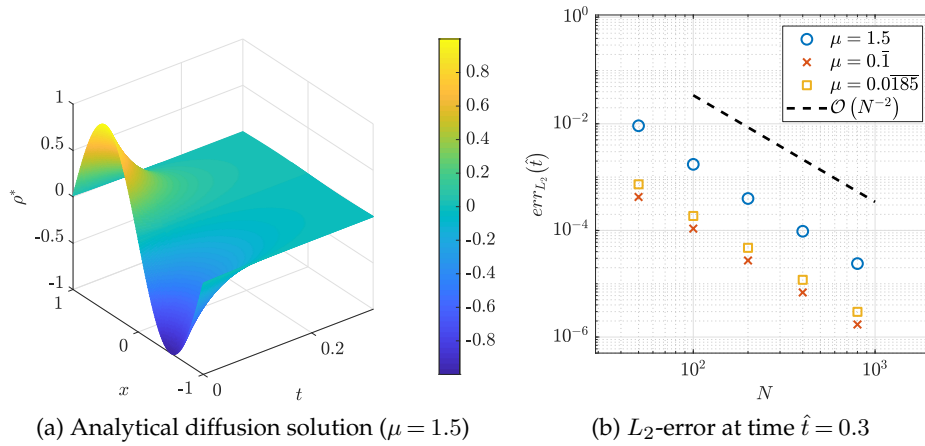


Figure 4: (a) Exemplary analytical solution (5.5) with $u = 0$ for $\mu = 1.5$, plotted until terminal time t_M . (b) L_2 -error at time $\hat{t} = 0.3$ for pure diffusion tests with $u_L = 0$ and parameters from Table 1.

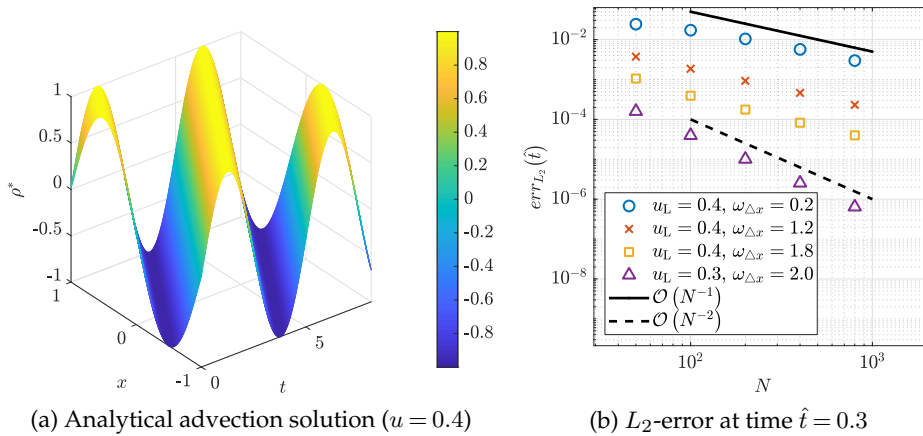
Table 3: Numerical errors for parabolically scaled LBM to approximate the diffusion equation (5.4) with $u = 0$, measured in terms of global error \overline{err} until terminal time t_M , local in time L_2 -error $err_{L_2}(\hat{t})$ at $\hat{t} = 0.3$, and experimental order of convergence (EOC).

N	$\mu = 1.5$		$\mu = 0.1$		$\mu = 0.0185$	
	$err_{L_2}(\hat{t})$	\overline{err}	$err_{L_2}(\hat{t})$	\overline{err}	$err_{L_2}(\hat{t})$	\overline{err}
50	0.00918773	0.02418652	0.00042383	0.00019562	0.00073274	0.00035212
100	0.00173503	0.00647128	0.00010807	0.00004982	0.00018672	0.00008982
200	0.00039696	0.00159275	0.00002729	0.00001257	0.00004714	0.00002267
400	0.00009645	0.00039637	0.00000686	0.00000317	0.00001184	0.00000569
800	0.00002387	0.00009897	0.00000172	0.00000079	0.00000297	0.00000143
EOC	2.1471	1.9832	1.9862	1.9867	1.9867	1.9865

(c) Hyperbolic conservation law

As noted in Section 3, the choice of hyperbolic scaling results in a hyperbolic conservation law as TEQ. For the numerical tests, the analytical solution to (5.4) with $\mu = 0$ is obtained by similarly setting $\mu = 0$ in (5.5). A visualization is provided in Figure 5a.

The corresponding simulation parameters from Table 4 yield first order convergence to the TEQ for $0 < \omega_{\Delta x} < 2$. Similar observations were found for a *D1Q2* LBE by Junk et al. [21]. Simulation results are summarized in Figure 5b and Table 5. Although the overall \overline{EOC} in Table 5 for $\omega_{\Delta x} = 0.2$ is lower than 1.0, the convergence speeds for two subsequent resolutions tend to 1.0 with increasing N . This trend can also be observed in Figure 5b, where an asymptotic alignment of the plotted error values for $\omega_{\Delta x} = 0.2$ to the first order reference line is clearly visible. A reason for the lowered order of convergence is already present in (3.7), where for hyperbolic scaling ($\gamma = 1$) the $\mathcal{O}(\epsilon)$ diffusion term arises intrinsically in the method's derivation (see Remark 3.1). Its fully discretized analogue is preceded by a modified factor [21], which on the one hand, grows inversely linear for $\omega_{\Delta x} \rightarrow 0$ and hence, for small $\omega_{\Delta x}$ slows down the first order along $\Delta x \rightarrow 0$. On the other hand, this modified factor is nulled out for $\omega_{\Delta x} = 2$, leading to second order convergence [21]. The latter limit case is included in 5b, where the optimal relaxation frequency approves the theoretical result from [21].



(a) Analytical advection solution ($u = 0.4$)

(b) L_2 -error at time $\hat{t} = 0.3$

Figure 5: (a) Exemplary analytical solution (5.5) with $\mu = 0$ for $u = 0.4$, plotted until terminal time $\hat{t}_M = 8.12$. (b) L_2 -error at time $\hat{t} = 0.3$ for pure advection tests with parameters from Table 4.

Table 4: Summary of hyperbolically scaled LBM discretization parameters (u_L denotes lattice units). Note that $u = u_L$.

N	hyperbolic scaling $\gamma = 1$		$u_L = 0.4$		$u_L = 0.3$	
	Δx	Δt	$\omega_{\Delta x}$	$\omega_{\Delta x}$	$\omega_{\Delta x}$	$\omega_{\Delta x}$
50	4×10^{-2}	4×10^{-2}	0.2	1.2	1.8	2.0
100	2×10^{-2}	2×10^{-2}	0.2	1.2	1.8	2.0
200	1×10^{-2}	1×10^{-2}	0.2	1.2	1.8	2.0
400	5×10^{-3}	5×10^{-3}	0.2	1.2	1.8	2.0
800	2.5×10^{-3}	2.5×10^{-3}	0.2	1.2	1.8	2.0

Stability-wise, the structural condition changes to a plain bound on the advection velocity $|u| < 0.\bar{3}$, which is comparable to a CFL condition [12,36]. The numerical tests approve the stability criterion, in the sense that with $\omega_{\Delta x} \rightarrow 2$, instabilities occur when $u = 0.4 > 0.\bar{3}$ (see Table 5). In the present setting, a complete blowup of the solution due to the violation of the stability bound appears solely for $t > \hat{t} = 0.3$ and $N > 50$.

Table 5: Numerical errors for hyperbolically scaled LBM to approximate the hyperbolic conservation law (5.4) with $\mu = 0$, measured in terms of global error \overline{err} until terminal time $\hat{t}_M = 8.12$, local in time L_2 -error $err_{L_2}(\hat{t})$ at $\hat{t} = 0.3$, and experimental order of convergence \overline{EOC} .

N	$\omega_{\Delta x} = 0.2$		$u_L = 0.4$ $\omega_{\Delta x} = 1.2$		$\omega_{\Delta x} = 1.8$		$u_L = 0.3$ $\omega_{\Delta x} = 2.0$	
	$err_{L_2}(\hat{t})$	\overline{err}	$err_{L_2}(\hat{t})$	\overline{err}	$err_{L_2}(\hat{t})$	\overline{err}	$err_{L_2}(\hat{t})$	\overline{err}
50	0.02439189	0.38400936	0.00374231	0.04888185	0.00105668	0.01053714	0.00015934	0.00076687
100	0.01721336	0.25267240	0.00185803	0.02560400	0.00039222	—	0.00003961	0.00022721
200	0.01040428	0.14837123	0.00092552	0.01311085	0.00017623	—	0.00001006	0.00005751
400	0.00569486	0.08146749	0.00046185	0.00663503	0.00008251	—	0.00000254	0.00001446
800	0.00297596	0.04289145	0.00023070	0.00333773	0.00003983	—	0.00000064	0.00000363
\overline{EOC}	0.7587	0.7906	1.0050	0.9681	1.1824	—	2.0201	1.9310

6. Conclusion

Based on the extension of an existing perturbation formalism, a constructive ansatz for the design of a 3×3 RS to approximate a scalar linear advection–diffusion equation was proposed. Subsequently, the equivalence to a $D1Q3$ DVBE was established. Structural stability was assessed along the way to obtain a sufficient criterion for stability of the fully discretized LBE. Finally, numerical tests approved the correctness of the derived stability bound. Further, overall second order convergence in space towards the TEQ was numerically investigated for the constructed LBM.

The novel constructive procedure outlined above, acts as a foundation for the algebraic characterization of DVM, utilized for example as DVBE in the derivation of LBM. It facilitates the joint treatment of RS and DVM in the first place, and furthermore decouples the LBM from the Maxwell–Boltzmann equilibrium and generalizes it to perturbation terms added to the TEQ. Generally speaking, the herein discussed linkage of the TRS and DVBE is based on construing the artificial variables and the corresponding perturbation terms in the RS as equilibrium moments for non-conserved (kinetic) variables in the DVMS. The construction of the LBM DVMS is done via a linear combination of the population functions f_i , which is initially arising from the moment summation (4.4), such that the reverse effect can be achieved by diagonalization of the DVMS, similar to spectrally decomposing the RS (see Figure 1). Hence, the conserved moments, generated from collision invariants, i.e. specific basis polynomials of C^* , in turn span the subspace of possible equilibrium operators for the DVBE. Henceforth, modifications of scaling parameters, perturbation coefficients, specific moments and artificial variables, effectuate the limit to distinct TEQ, and finally yield control over the terms appearing in the PDE which is to be approximated.

The equivalencies of RS and DVMS, as well as TRS and DVBE, lead to a better understanding of the similarities between mathematical results obtained in the more general field of RS and the specific achievements on the theoretical background of LBM. Current investigations include the *a priori* determination of specific equilibria for reaching distinct types of generic, possibly multi-dimensional TEQ with DVBM and LBM, and further, an accuracy analysis to frame the interlacing of perturbation coefficients and discretization parameters in the relaxation limit.

Data Accessibility. This article has no additional data.

Authors' Contributions. SS conceived, conducted and documented the study. MF gave the initial thoughts behind the proposed perturbation ansatz. MF and MJK supervised the research. All authors read and approved the manuscript.

Competing Interests. The authors declare that they have no competing interests.

Funding. This work was partially funded by the "Deutsche Forschungsgemeinschaft" (DFG, KR4259.6-1, PBRsim).

Acknowledgements. SS would like to thank Willy Dörfler from the Institute for Applied and Numerical Mathematics at the Karlsruhe Institute of Technology, for providing the work facilities and excellent supervision, as well as for pointing out highly valuable references.

References

1. AREGBA-DRIOLLET, D., AND NATALINI, R.
Discrete kinetic schemes for multidimensional systems of conservation laws.
SIAM Journal on Numerical Analysis 37, 6 (2000), 1973–2004.
2. BANDA, M. K., YONG, W.-A., AND KLAR, A.
A stability notion for lattice Boltzmann equations.
SIAM Journal on Scientific Computing 27, 6 (2006), 2098–2111.
3. BHATNAGAR, P., GROSS, E. P., AND KROOK, M.
A model for collisional processes in gases i: small amplitude processes in charged and in neutral one-component systems.
Physical Review 94 (1954), 511–525.
4. BIANCHINI, R.
Uniform asymptotic and convergence estimates for the Jin–Xin model under the diffusion scaling.
SIAM Journal on Mathematical Analysis 50, 2 (2018), 1877–1899.
5. BOUCHUT, F.
Construction of BGK models with a family of kinetic entropies for a given system of conservation laws.
Journal of Statistical Physics 95, 1-2 (1999), 113–170.
6. BOUCHUT, F.
Stability of relaxation models for conservation laws.
In *European Congress of Mathematics* (2005), European Mathematical Society, pp. 95–101.
7. BOUCHUT, F., GUARGUAGLINI, F. R., AND NATALINI, R.
Diffusive BGK approximations for nonlinear multidimensional parabolic equations.
Indiana University Mathematics Journal (2000), 723–749.
8. CAETANO, F., DUBOIS, F., AND GRAILLE, B.
A result of convergence for a mono-dimensional two-velocities lattice Boltzmann scheme.
arXiv preprint arXiv:1905.12393v1 [math.AP] (2019).
9. CHOPARD, B., FALCONE, J.-L., AND LATT, J.
The lattice Boltzmann advection-diffusion model revisited.
The European Physical Journal Special Topics 171, 1 (2009), 245–249.
10. COREIXAS, C., CHOPARD, B., AND LATT, J.
Comprehensive comparison of collision models in the lattice Boltzmann framework: Theoretical investigations.
Phys. Rev. E 100 (Sep 2019), 033305.
11. DELLAR, P. J.
An interpretation and derivation of the lattice Boltzmann method using Strang splitting.
Computers & Mathematics with Applications 65, 2 (2013), 129–141.
12. DUBOIS, F., GRAILLE, B., AND RAO, S. V. R.
A stability property for a mono-dimensional three velocities scheme with relative velocity.
arXiv preprint arXiv:1911.12215v1 [math.AP] (2019).
13. GAEDTKE, M., WACHTER, S., RÄDLE, M., NIRSCHL, H., AND KRAUSE, M. J.
Application of a lattice Boltzmann method combined with a Smagorinsky turbulence model to spatially resolved heat flux inside a refrigerated vehicle.
Computers & Mathematics with Applications 76, 10 (2018), 2315–2329.

14. GRAILLE, B.
Approximation of mono-dimensional hyperbolic systems: A lattice Boltzmann scheme as a relaxation method.
Journal of Computational Physics 266 (2014), 74–88.
15. HAUSSMANN, M., SIMONIS, S., NIRSCHL, H., AND KRAUSE, M. J.
Direct numerical simulation of decaying homogeneous isotropic turbulence – numerical experiments on stability, consistency and accuracy of distinct lattice Boltzmann methods.
International Journal of Modern Physics C 30, 09 (2019), 1–29.
16. HE, X., AND LUO, L.-S.
Theory of the lattice Boltzmann method: From the Boltzmann equation to the lattice Boltzmann equation.
Phys. Rev. E 56 (Dec 1997), 6811–6817.
17. JIN, S., AND LIU, H.
Diffusion limit of a hyperbolic system with relaxation.
Methods and Applications of Analysis 5, 3 (1998), 317–334.
18. JIN, S., AND XIN, Z.
The relaxation schemes for systems of conservation laws in arbitrary space dimensions.
Communications on pure and applied mathematics 48, 3 (1995), 235–276.
19. JUNK, M.
On the construction of discrete equilibrium distributions for kinetic schemes.
Institut für Techno- und Wirtschaftsmathematik Kaiserslautern, ITWM Report 14 (1999).
20. JUNK, M., KLAR, A., AND LUO, L.-S.
Asymptotic analysis of the lattice Boltzmann equation.
Journal of Computational Physics 210, 2 (2005), 676–704.
21. JUNK, M., AND RHEINLANDER, M. K.
Regular and multiscale expansions of a lattice Boltzmann method.
Progress in Computational Fluid Dynamics, an International Journal 8, 1-4 (2008), 25–37.
22. JUNK, M., AND YANG, Z.
 L^2 Convergence of the lattice Boltzmann method for one dimensional convection-diffusion-reaction equations.
Communications in Computational Physics 17, 5 (2015), 1225–1245.
23. JUNK, M., AND YONG, W.-A.
Weighted L^2 -stability of the lattice Boltzmann method.
SIAM Journal on Numerical Analysis 47, 3 (2009), 1651–1665.
24. KRAUSE, M. J.
Fluid flow simulation and optimisation with lattice Boltzmann methods on high performance computers: application to the human respiratory system.
PhD thesis, Karlsruhe Institute of Technology (KIT), 2010.
25. KRÜGER, T., KUSUMAATMAJA, H., KUZMIN, A., SHARDT, O., SILVA, G., AND VIGGEN, E. M.
The lattice Boltzmann method.
Springer International Publishing 10 (2017), 978–3.
26. LEVEQUE, R. J.
Finite difference methods for ordinary and partial differential equations: steady-state and time-dependent problems, vol. 98.
Siam, 2007.
27. LIU, T.-P.
Hyperbolic conservation laws with relaxation.
Communications in Mathematical Physics 108, 1 (1987), 153–175.
28. MINK, A., THÄTER, G., NIRSCHL, H., AND KRAUSE, M. J.
A 3D lattice Boltzmann method for light simulation in participating media.
Journal of Computational Science 17 (2016), 431–437.
29. MOHAMAD, A. A.
Lattice Boltzmann Method, vol. 70.
Springer, 2011.
30. MOJTABI, A., AND DEVILLE, M. O.
One-dimensional linear advection–diffusion equation: Analytical and finite element solutions.
Computers & Fluids 107 (2015), 189–195.

31. MORTON, K. W.
Numerical Solution of Convection-Diffusion Problems.
Chapman & Hall, 1996.
32. OTTE, P., AND FRANK, M.
Derivation and analysis of lattice Boltzmann schemes for the linearized Euler equations.
Computers & Mathematics with Applications 72, 2 (2016), 311–327.
33. OTTE, P., AND FRANK, M.
A structured approach to the construction of stable linear lattice Boltzmann collision operator.
Computers & Mathematics with Applications, in press (2019).
34. RAO, R., AND SUBBA RAO, M.
A simple multidimensional relaxation scheme based on characteristics and interpolation.
In *16th AIAA Computational Fluid Dynamics Conference* (2003), p. 3535.
35. RHEINLÄNDER, M. K.
Analysis of Lattice-Boltzmann Methods: Asymptotic and Numeric Investigation of a Singularly Perturbed System.
PhD thesis, Universität Konstanz, 2007.
36. RHEINLÄNDER, M. K.
Stability and multiscale analysis of an advective lattice Boltzmann scheme.
Progress in Computational Fluid Dynamics (PCFD) 8, 1-4 (2008), 56–68.
37. RHEINLÄNDER, M. K.
On the stability structure for lattice Boltzmann schemes.
Computers & Mathematics with Applications 59, 7 (2010), 2150–2167.
38. SHEN, W., ZHANG, C., AND ZHANG, J.
Relaxation method for unsteady convection–diffusion equations.
Computers & Mathematics with Applications 61, 4 (2011), 908–920.
39. SUGA, S.
Numerical schemes obtained from lattice Boltzmann equations for advection diffusion equations.
International Journal of Modern Physics C 17, 11 (2006), 1563–1577.
40. TREFETHEN, L. N.
Finite difference and spectral methods for ordinary and partial differential equations.
Cornell University - Department of Computer Science and Center for Applied Mathematics, 1996.
41. UBERTINI, S., ASINARI, P., AND SUCCI, S.
Three ways to lattice Boltzmann: A unified time-marching picture.
Phys. Rev. E 81 (Jan 2010), 016311.
42. WEISS, J.-P.
Numerical analysis of lattice Boltzmann methods for the heat equation on a bounded interval.
Univ.-Verlag Karlsruhe, 2006.
43. YONG, W.-A.
Basic aspects of hyperbolic relaxation systems.
In *Advances in the theory of shock waves.* Springer, 2001, pp. 259–305.
44. YONG, W.-A.
An onsager-like relation for the lattice Boltzmann method.
Computers & Mathematics with Applications 58, 5 (2009), 862–866.